Direct Experimental Observation of a New Mechanism for Sputtering of Solids by a Large Polyatomic Projectile: Velocity-Correlated Cluster Emission

E. Armon, A. Bekkerman, Y. Cohen, J. Bernstein, B. Tsipinyuk, and E. Kolodney
Schulich Faculty of Chemistry, Technion—Israel Institute of Technology, Haifa 32000, Israel
(Received 21 November 2013; published 11 July 2014)

We have measured kinetic energy distributions of $Ta_nC_n^+$ ($n = 1$–10) and Ag_n^+ ($n = 1$–9) cluster ions sputtered off Ta and Ag targets, following impact of C_{60}^- at 14 keV kinetic energy. A gradual increase of the most probable kinetic energies with increased size of the emitted cluster was observed (nearly the same velocity for all n values). This behavior is in sharp contrast to that reported for cluster emission induced by the impact of a *monoatomic* projectile. Our observation is in good agreement with a mechanism based on the new concept of a superhot moving precursor as the source of the emitted clusters.

DOI: 10.1103/PhysRevLett.113.027604 PACS numbers: 79.20.Rf, 34.35.+a, 68.49.Df, 68.49.Sf

The emission of particles (atoms or clusters) off a solid material due to ion bombardment (sputtering) is a process of both fundamental and practical importance in many fields and applications [1]. Sputtering-related phenomena include, for example, the impact-induced formation of periodic erosion patterns (self-organized) at the nanoscale [2,3], enhanced sputtering of nanostructures associated with the explosive ejection of large clusters [4], surface smoothing [5], growth of nanostructured surfaces from size-selected cluster ions [6], and mechanisms of microscopic to mesoscopic crater formation [7,8]. The last one is also relevant for analyzing erosion features of exposed surfaces of a spacecraft [9], or natural astronomical objects [10], due to impact of hypervelocity interstellar dust nanograins, and sputtering erosion inside ion thrusters [11]. Leading applications include nanoscale surface processing and analysis techniques such as focused ion beams (FIB) and secondary ion mass spectrometry (SIMS).

The main recent interest regarding fundamental aspects is related with differences between the characteristics of sputtering induced by polyatomic or cluster projectiles as compared with that induced by atomic projectiles [7,8,12–24]. This also reflects an increasing interest in new cluster-surface impact phenomena in general [24]. For atomic projectiles, sputtering theory can be considered as well established. A fairly good understanding of the underlying mechanisms was gained, in terms of linear collision cascades [25–28] or various thermal spike models [27–30]. In contrast, mechanisms of particle emission following bombardment with polyatomic ions are generally poorly understood. Enhanced yield of sputtered atomic and particularly cluster ions [15–18] and neutrals [19,20] under transition from atomic to molecular (cluster) ion bombardment is usually associated with a highly nonlinear cascade regime. There is a rather small number of studies where kinetic energy distributions (KEDs) of sputtered cluster ions [15–18,31,32] or neutrals [19,20] were measured under bombardment of solids by molecular (cluster) ions. Molecular dynamics (MD) simulations provided deeper insight into the evolution of the collisional spike, formed under either heavy atom or cluster impact [21–23,33–37] and resulting in clusters emission. Here we present a direct experimental evidence for a novel sputtering phenomenon which was not yet reported either experimentally or computationally. It is based on the unique behavior observed for KEDs of surface emitted clusters following impact by a large polyatomic projectile (C_{60}^-). We rationalize our results in terms of a novel sputtering mechanism where an outgoing, moving precursor, is the source of the emitted clusters.

A detailed description of the experimental setup is available elsewhere [38]. Briefly, a beam of C_{60}^- negative ions was accelerated to 14 keV and collided with an atomically clean (sputter-annealed) polycrystalline tantalum and silver targets. During measurements the C_{60}^- ion beam (5–7 nA, 30 μm beam spot diameter) was rastered over a target area of 0.5×0.5 mm^2. Mass resolved KEDs of sputtered ions were measured by a quadrupole mass spectrometer equipped with a homemade on-axis retarding field energy analyzer (RFA) with energy resolution $\Delta E = 0.4$ eV. Incidence angle of the C_{60}^- ion beam was 45°. The sputtered ions were collected along the normal into the mass spectrometer using a weak extraction potential (25 V) which provided good signal-to-noise ratio while keeping the effect of the extraction field on the KEDs rather small. This field effect can be related with metastability of the outgoing species (on-flight delayed electron emission or the less probable—at least for the case of tantalum carbide clusters—unimolecular fragmentation) and angular dependence of the KEDs. We have found that the extraction field induces some shift and small distortion of the KEDs but does not change the results meaningfully (see below for details). Calibration of the kinetic energy axis was verified using thermally emitted (surface ionized) K^+ ions accelerated towards the RFA.

The first material to be studied was tantalum carbide. We have found that the impact of C_{60}^- on tantalum provides an effective way for the *in situ* growth of a 1:1 (Ta:C) stoichiometric layer [39]. Nearly complete ionization is expected for hot neutral Ta_nC_m clusters with $n \geq 4$. This is based on similar observation for pure Ta_n clusters [40] and the low ionization energies of the Ta_nC_m clusters (≤ 5.5 eV [41]) as compared with their high stability against fragmentation [42]. The measurements started with the irradiation of the tantalum target with C_{60}^- beam while following the competitive growth and erosion kinetics of the carbidic TaC layer (e.g. buildup of the $Ta_4C_4^+$ signal) until steady state saturation is achieved. Bright field transmission electron microscope image of the film as well as FFT diffraction pattern revealed that the steady state film is composed of densely packed face centered cubic TaC nanocrystallines with 3–4 nm typical size (measured lattice spacing 0.257 nm corresponding to the (111) plane) [39]. The steady state positive ions mass spectrum was composed of groups of $Ta_nC_m^+(n = 1–10)$ cluster ions, each nearly symmetric with respect to the central $n = m$ peak. Due to the complete coverage of the Ta substrate with TaC crystallites, pure Ta_n^+ clusters were detectable only up to $n = 3$.

Figure 1(a) presents KEDs of emitted $Ta_nC_n^+(n = 1–9)$ ions following impact of 14 keV C_{60}^- on the in situ grown TaC layer. Two main features are evident: (1) the most probable energies E_{mp} are gradually shifted to higher values with increase in cluster size, and (2) the distributions are getting broader with cluster size. A pure Ta^+ KED (triangles) is also given for comparison and shown to be the narrowest as compared with the $Ta_nC_n^+$ KEDs. The intensity of Ta_2^+ and Ta_3^+ was too low to allow their KEDs to be measured. The apparent negative energy tail observed for the small clusters ($n = 1, 2$) points at some contribution of metastability (unimolecular decomposition or thermally delayed electron emission) along the flight path. For $n \geq 3$ this contribution can be considered as negligible. The trends observed of increasing E_{mp} values and distributions width with n are in sharp contrast to the behavior of KEDs consistently reported in the literature for both neutral and ionized clusters emission using keV *atomic* projectiles [18,20,31,32,43,44]. In order to verify reproducibility of these literature results we have measured KEDs of $Ta_n^+(n = 1–9)$ sputtered from clean tantalum by Cs^+ ions at 14 keV [Fig. 1(b)]. The observed broad high energy KEDs of the monomers and gradual narrowing and shift to lower energies with n of the KEDs of the Ta_n^+ clusters, are in good agreement with all earlier measurements using atomic projectiles. We have measured the observed effect with a C_{60}^- projectile (increase of E_{mp} values with increase of cluster size n, as in Figs. 1(a) and Fig. 2) under different extraction voltages (up to 100 eV) and found that this effect is actually getting more pronounced when we reduce the field. Namely, the observed phenomenon is clearly not field induced.

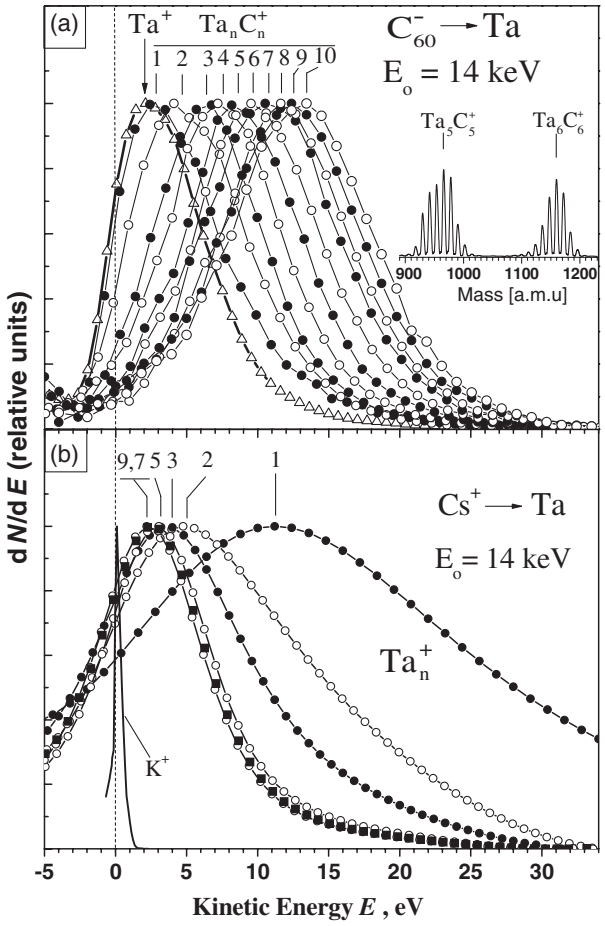

FIG. 1. (a) Measured KEDs of $Ta_nC_n^+(n = 1–10)$ cluster ions sputtered from TaC layer by C_{60}^- impact. Insert shows a representative part of the mass spectrum. (b) Kinetic energy distributions of $Ta_n^+(n = 1–9)$ cluster ions sputtered from a tantalum target by Cs^+ impact.

The gradual increase of E_{mp} and width for the KEDs of sputtered cluster ions under C_{60}^- bombardment are also in contrast to the results reported earlier for atomic and cluster ions sputtered by small but heavy gold cluster projectiles [15–18]. Comparison with reported KEDs for neutral monomer and dimer emission [19,20] will be discussed later.

Inspection of the KEDs following the impact of C_{60}^- ions (Fig. 1) shows that all clusters share a nearly common most probable velocity (roughly the same differences between E_{mp} values of adjacent KEDs, especially for $n \geq 3$). Since impact conditions are well within the nonlinear spike regime [27], we assume that the source of the emitted clusters is some kind of a superhot precursor species (with temperature T) moving with a center-of-mass (c.m.) velocity $V_{c.m.}$. Within our simplistic model, we view the outgoing precursor as an ensemble of temporarily organized but weakly interacting Ta_nC_m clusters. Assuming a Maxwellian velocity distribution for the different Ta_nC_n groups *within* the precursor species (in its c.m. frame) one

can write a flux velocity distribution for the Ta_nC_n groups dN_n/dV in the laboratory frame within a small solid angle $\Delta\Omega$,

$$\frac{dN_n}{dV} = A(nm)^{3/2}V^3 \exp\left[-\frac{nm(V - V_{\text{c.m.}})^2}{2kT}\right], \quad (1)$$

where $A = n_o\Delta\Omega/(2\pi kT)^{3/2}$, k is the Boltzmann constant, n_o is the volume density of the Ta_nC_n groups, and m is the mass of a TaC unit. The corresponding flux energy distribution in the laboratory frame is given by

$$\frac{dN_n}{dE} = 2A(nm)^{-1/2}E \exp\left[-\frac{(\sqrt{E} - \sqrt{n\varepsilon})^2}{kT}\right], \quad (2)$$

where $\varepsilon = mV_{\text{c.m.}}^2/2$ is the kinetic energy of a TaC unit moving with the precursor c.m. velocity $V_{\text{c.m.}}$.

The calculated KEDs [Eq. (2)] are presented in Fig. 2(a) along with the measured KEDs taken from Fig. 1(a) for $Ta_nC_n^+(n = 3–7)$. A good agreement is obtained (excluding part of the low energy side of the distributions) using a uniquely best fitted pair of ε, kT parameters with the values $kT = 1.25 \pm 0.09$ eV and $\varepsilon = 1.16 \pm 0.06$ eV (corresponding $V_{\text{c.m.}} = 1074 \pm 28$ m sec^{-1}).

The variation of the most probable energy E_{mp} with cluster size n as derived from Eq. (2) is given by

$$E_{\text{mp}}(n) = \frac{n \cdot \varepsilon}{4}\left(1 + \sqrt{1 + \frac{4kT}{n \cdot \varepsilon}}\right)^2. \quad (3)$$

For large values of n such that $n \cdot \varepsilon \gg 4kT$ one gets the asymptotic form of $E_{\text{mp}}(n)$as

$$E_{\text{mp}}(n) = n \cdot \varepsilon + 2kT \quad (4)$$

Figure 2(b) presents measured and calculated $E_{\text{mp}}(n)$ values and dependences correspondingly, using the best fitted ε and kT parameters. A good agreement is demonstrated ($n = 1–10$). The comparison between the $E_{\text{mp}}(n) = n \cdot \varepsilon$ (T = 0 limit) as shown in Fig. 2(b) and the asymptotic Eq. (4) emphasizes the importance of the thermal contribution. For the sake of clarity, additional presentations of the data in comparison with model predictions are given in the Supplemental Material [45].

We would like now to discuss the possible nature of the precursor state. It is assumed that the impacting C_{60}^- generates an extremely energy dense (superhot) nanovolume, slightly below the surface [21,22]. There is a buildup of an extreme high pressure within this sub-surface impact zone, eventually pushing the topmost surface layers outward [7]. The observed common c.m. velocity $V_{\text{c.m.}}$, for all emitted clusters, implies a correlated upward motion as an ensemble of tightly confined species composed of the uppermost atomic layers of the target. We describe this collectively outward moving superhot ensemble as the

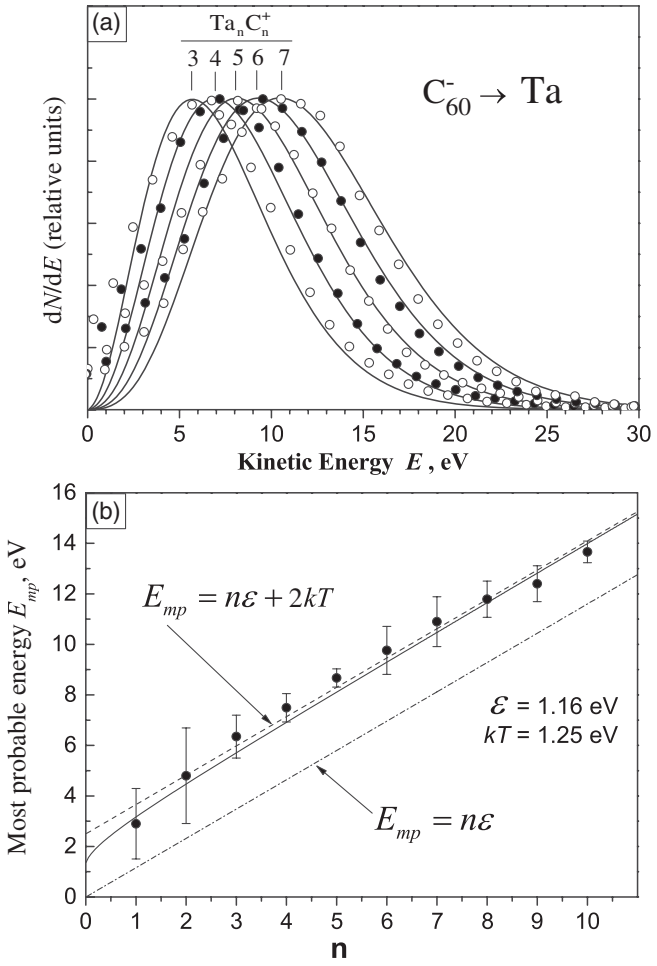

FIG. 2. Analysis of the measured $Ta_nC_n^+$ KEDs based on a fit to a shifted Maxwell distribution [Eq. (2)]. (a) Measured KEDs are given by solid and empty circles. Shifted Maxwell distributions fitted with a single pair of parameters ($\varepsilon = 1.16$ eV, $kT = 1.25$ eV) are given by the solid lines. (b) Measured and calculated E_{mp} values vs cluster size n. The measured values are given by solid circles. The solid line is given by Eq. (3), the dashed line by Eq. (4), and the dash-dotted line is E_{mp} in the $T = 0$ limit.

precursor state. The precise nature of the precursor, its formation conditions and the specific stage during spike evolution at which it is being defined, are still not clear. The two limiting cases we consider are (1) partially detached precursor (still subsurface or just bulging out) where the fragments are emitted directly from the surface or (2) fully surface-detached large cluster (up to a few nanometers away from the surface) which fragments within a few psec after leaving the surface. The fitted temperature value may be somewhat too high (from the point of view of thermally activated fragmentation dynamics) but we note that the precursor temperature T is treated here as a translational one. It does not necessarily imply also a vibrational temperature of the cluster constituents of the precursor since vibrational-translational equilibration may not yet be

achieved within a possible scenario involving the ultrashort time scale of the initial phase of the spike (≤ 1 psec).

Correlated or collective upward motion of a rather large number of atoms of the few topmost layers just above the core of the spike was observed in MD simulations by several groups [21–23,32–37]. Emission of large clusters containing up to several tens of atoms [33,46] and micro-explosion events [34] leading to emission of clusters containing up to ~100 atoms were also observed. Such moving large hot clusters may well be considered as another precursor variant. However, to our knowledge, the velocity correlated cluster emission effect as measured here (shifted Maxwell KEDs for $n \geq 3$) was not yet observed in MD simulations (which are very sensitive to the potential used [23]).

We have also carried out measurements of C_{60}^- impact induced sputtering of a silver target, having a much lower cohesive energy and considerably higher thermal conductivity as compared with tantalum carbide. As shown in Fig. 3(a), we were able to measure KEDs of emitted Ag_n^+ up to $n = 9$. Mixed silver-carbon clusters were observed only up to $Ag_3C_5^+$ with absolutely no buildup of a carbide layer. Similarly to the $Ta_nC_n^+$ KEDs, the most pronounced features of the Ag_n^+ KEDs are a gradual shift of E_{mp} to higher values and a corresponding broadening with increase in cluster size n. For comparison, we have also measured KEDs of Ag_n^+ sputtered by a monoatomic projectile (5 keV Ar^+ ions). As expected, these KEDs exhibited the opposite trend (gradual narrowing and shift to lower energies for $n = 1$–7). The measured Ag_n^+ KEDs in Fig. 3(a) (C_{60}^- projectile) could be reasonably well fitted with a shifted Maxwellian [Eq. (2)] using a single ε, kT pair only for $n \geq 5$ and mainly for the peak value and high energy side of the distribution. Calculated KEDs using the best fitted values $kT = 1.13 \pm 0.10$ eV and $\varepsilon = 0.40 \pm 0.03$ eV are given by the solid line. E_{mp} values of measured $Ag_n^+(n = 1$–$9)$ KEDs are presented in Fig. 3(b) as a function of n (solid circles) along with the calculated E_{mp} values [Eq. (3)]. A rather good agreement is obtained for $n \geq 3$. However, E_{mp} (Ag_2^+) deviates appreciably from the common velocity line [Eq. (3)] with $E_{mp}(Ag_2^+)/E_{mp}(Ag^+) \sim 3$.

A common velocity type emission was reported earlier also for neutral In and In_2 sputtered off an indium target (Au_2^-, Au_3^- projectiles at 10 keV), peaking at exceptionally low energies (0.1–0.2 eV) [19], and Ag, Ag_2 sputtered off a silver target (C_{60}^+ projectile at 10–20 keV) peaking at energies of 0.75–1.5 eV [20]. This behavior was attributed to an adiabatic free jetlike expansion of the ejecta [20]. The measured KEDs of the emitted Ag, Ag_2 were reproduced in MD simulations [21]. Even if one assumes that the free jetlike interpretation is applicable, under certain conditions, to the sputtering of small clusters ($n \leq 3$) from relatively weakly bound metals such as silver and indium, it certainly cannot explain the emission of superhot, high (common) velocity large clusters as observed here. Gas dynamic acceleration and resulting velocities unification of emitted clusters under free jet (nozzle) expansion conditions will strongly degrade with increase of mass of the "seeded" clusters as compared with that of the "carrier gas "(i.e., enhanced velocity slip effect for heavier clusters [47–49]). Our results show no such behavior. As is clearly shown in Figs. 2 and 3, all clusters share a common $V_{c.m.}$ velocity. However, taking into account the deviation of $E_{mp}(Ag_2^+)$ from the common velocity line [see Fig. 3(b)], it is quite possible that under our experimental conditions there is an additional mechanism contributing to the emission of Ag_2^+ which is different from the one responsible for the emission of the larger Ag_n^+ $(n \geq 3)$ clusters. In the Supplemental Material [45] we show that the possibility that this

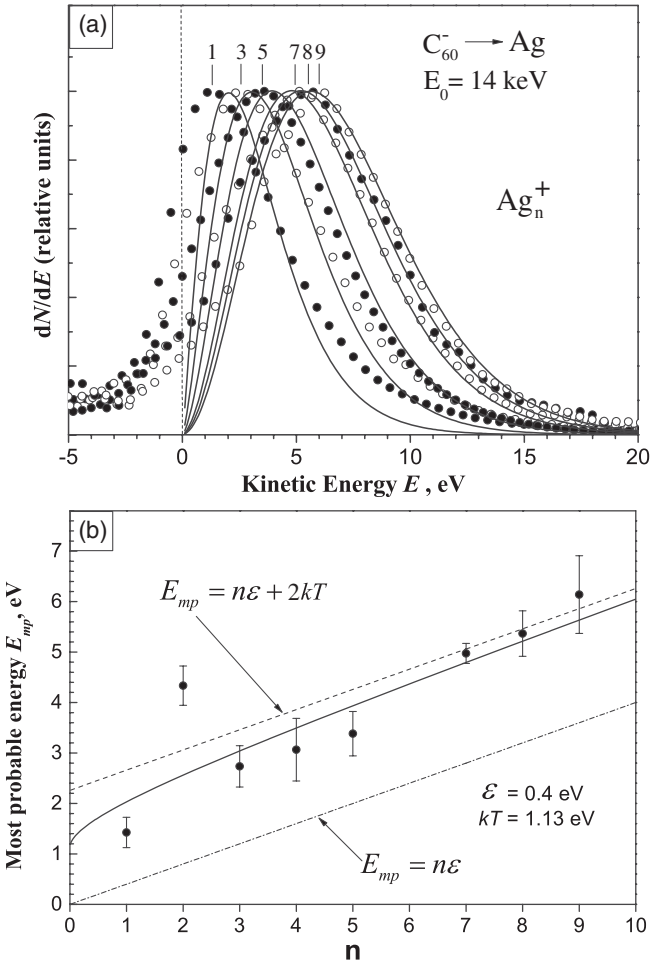

FIG. 3. Measured and calculated KEDs of $Ag_n^+(n = 1$–$9)$ cluster ions sputtered from a silver target by C_{60}^- impact. (a) Measured KEDs are given by solid and empty circles. Shifted Maxwell distributions [see Eq. (2)] fitted with a single pair of parameters ($\varepsilon = 0.40$ eV,$kT = 1.13$ eV) are given by the solid lines. (b) Measured and calculated E_{mp} values vs cluster size n. The measured values are given by solid circles. The solid line is given by Eq. (3), the dashed line by Eq. 4, and the dash-dotted line is E_{mp} in the $T = 0$ limit.

additional mechanism can be described in terms of a free jetlike expansion (as proposed for neutral Ag, Ag_2 sputtered by C_{60}^+ (vs Ga^+) [20]) is questionable.

In summary, based on a direct experimental observation of the KEDs of sputtered cluster ions, we propose a new mechanism for the sputtering of solid surfaces by a large polyatomic projectile (C_{60}^-). According to this mechanism, a superhot moving precursor is the source of the emitted clusters. The central observation that all clusters emitted from a given target, $Ta_nC_n^+$ ($n = 1$–10) from tantalum carbide and Ag_n^+ ($n = 1$–9) from silver, share a nearly common most probable velocity, is in a striking contrast to the corresponding behavior of cluster emission induced by a monoatomic ion impact. The general nature of this new sputtering phenomenon is demonstrated for two very different types of target materials. We expect it to have implications for impact cratering and erosion of surfaces using large cluster projectiles.

The research was supported by the German-Israeli Binational James-Franck Minerva program.

[1] R. Behrisch and W. Eckstein, *Sputtering by Particle Bombardment.* Topics in Applied Physics Vol. 110 (Springer-Verlag, Berlin, 2007).
[2] R. M. Bradley and P. D. Shipman, Phys. Rev. Lett. **105**, 145501 (2010).
[3] P. Karmakar, G. F. Liu, Z. Sroubek, and J. A. Yarmoff, Phys. Rev. Lett. **98**, 215502 (2007).
[4] G. Greaves, J. A. Hinks, P. Busby, N. J. Mellors, A. Ilinov, A. Kuronen, K. Nordlund, and S. E. Donnelly, Phys. Rev. Lett. **111**, 065504 (2013).
[5] N. Toyoda, N. Hagiwara, J. Matsuo, and I. Yamada, Nucl. Instrum. Methods Phys. Res., Sect. B **161**, 980 (2000).
[6] R. E. Palmer, S. Pratontep, and H.-G. Boyen, Nat. Mater. **2**, 443 (2003).
[7] J. Samela and K. Nordlund, Phys. Rev. Lett. **101**, 027601 (2008).
[8] C. Anders, E. M. Bringa, G. Ziegenhain, G. A. Graham, J. F. Hansen, N. Park, N. E. Teslich, and H. M. Urbassek, Phys. Rev. Lett. **108**, 027601 (2012).
[9] F. Hörz *et al.*, Science **314**, 1716 (2006).
[10] R. E. Johnson, *Energetic Charged-Particle Interactions with Atmospheres and Surfaces.* (Springer, Berlin, 1990).
[11] D. M. Goebel and I. Katz, "*Fundamentals of Electric Propulsion: Ion and Hall Thrusters*" (John Wiley & Sons, Hoboken, NJ, 2008).
[12] C. Anders and H. M. Urbassek. Phys. Rev. Lett. **99**, 027602 (2007).
[13] R. D. Rickman, S. V. Verkhoturov, E. S. Parilis, and E. A. Schweikert. Phys. Rev. Lett. **92**, 047601 (2004).
[14] C. Szakal, J. Kozole, M. F. Russo, Jr, B. J. Garrison, and N. Winograd, Phys. Rev. Lett. **96**, 216104 (2006).
[15] S. F. Belykh, U. Kh. Rasulev, A. V. Samartsev, and I. V. Veryovkin, Nucl. Instrum. Methods Phys. Res., Sect. B **136–138**, 773 (1998).
[16] S. F. Belykh, B. Habets, U. Kh. Rasulev, A. V. Samartsev, L. V. Stroev, and I. V. Veryovkin, Nucl. Instrum. Methods Phys. Res., Sect. B **164–165**, 809 (2000).
[17] S. N. Morozov and U. K. Rasulev, Nucl. Instrum. Methods Phys. Res., Sect. B **203**, 192 (2003).
[18] I. V. Veryovkin, S. F. Belykh, A. Adriaens, and F. Adams, Nucl. Instrum. Methods Phys. Res., Sect. B **219–220**, 215 (2004); I. V. Veryovkin, S. F. Belykh, A. Adriaens, A. V. Zinovev, and F. Adams, Appl. Surf. Sci. **231–232**, 101 (2004).
[19] A. V. Samartsev, A. Duvenbeck, and A. Wucher, Phys. Rev. B **72**, 115417 (2005).
[20] S. Sun, C. Szakal, N. Winograd, and A. Wucher, J. Am. Soc. Mass Spectrom. **16**, 1677 (2005)
[21] Z. Postawa, B. Czerwinski, M. Szewczyk, E. J. Smiley, N. Winograd, and B. J. Garrison, J. Phys. Chem. B **108**, 7831 (2004).
[22] T. J. Colla, R. Aderjan, R. Kissel, and H. M. Urbassek, Phys. Rev. B **62**, 8487 (2000).
[23] T. J. Colla and H. M. Urbassek, Nucl. Instrum. Methods Phys. Res., Sect. B **164–165**, 687 (2000).
[24] V. Popok, I. Barke, E. E. B. Campbell, and K.-H. Meiwes-Broer, Surf. Sci. Rep. **66**, 347 (2011).
[25] P. Sigmund, Phys. Rev. **184**, 383 (1969); **187**, 768 (1969).
[26] M. Thompson, Philos. Mag. **18**, 377 (1968).
[27] H. M. Urbassek, K. Dan. Vidensk. Selsk. Mat. Fys. Medd. **52**, 433 (2006).
[28] A. Wucher, K. Dan. Vidensk. Selsk. Mat. Fys. Medd. **52**, 405 (2006).
[29] P. Sigmund and C. Claussen, J. Appl. Phys. **52**, 990 (1981).
[30] M. Urbassek, in *Sputtering by Particle Bombardment*, Topics in Applied Physics Vol. 110, edited by R. Behrisch and W. Eckstein (Springer-Verlag, Berlin, 2007), p. 189.
[31] G. Betz and K. Wien, Int. J. Mass Spectrom. Ion Process. **140**, 1 (1994).
[32] H. Gnaser, in *Sputtering by Particle Bombardment*, Topics in Applied Physics Vol. 110, edited by R. Behrisch and W. Eckstein (Springer-Verlag, Berlin, 2007), p. 231.
[33] G. Betz and W. Husinsky, Phil. Trans. R. Soc. A **362**, 177 (2004).
[34] R. S. Averback and M. Ghaly, Nucl. Instrum. Methods Phys. Res., Sect. B **127–128**, 1 (1997).
[35] M. Ghaly, K. Nordlund, and R. S. Averback, Philos. Mag. A **79**, 795 (1999).
[36] K. Nordlund, J. Keinonen, M. Ghaly, and R. S. Averback, Nucl. Instrum. Methods Phys. Res., Sect. B **148**, 74 (1999).
[37] H. M. Urbassek and K. T. Waldeer, Phys. Rev. Lett. **67**, 105 (1991).
[38] Y. Cohen, V. Bernshtein, E. Armon, A. Bekkerman, and E. Kolodney, J. Chem. Phys. **134**, 124701 (2011).
[39] Y. Cohen, E. Armon, M. Baskin, and E. Kolodney (to be published).
[40] R. Heinrich, C. Staudt, M. Wahl, and A. Wucher, in *Proceedings of the 12th International Conference on SIMS, Brussels, Belgium, 1999*, edited by A. Benninghoven, P. Bertrand, H.-N. Migeon, and H. W. Werner, 2000, p. 111.
[41] V. Dryza, M. A. Addicoat, Jason R. Gascooke, M. A. Buntine, and G. F. Metha, J. Phys. Chem. A, **109**, 11180 (2005).
[42] J. Bernstein and E. Kolodney (unpublished). Density functional theory calculations were carried out for a representative cluster ($Ta_9C_9^+$) based on optimal ground

state structures. For the emission of TaC (decay to $Ta_8C_8^+$) we have obtained $\Delta E = 10.5$ eV. For the emission of a Ta atom (decay to $Ta_8C_9^+$) we have obtained $\Delta E = 10.6$ eV.

[43] Z. Ma, W. F. Calaway, M. J. Pellin, and E. I. von Nagy-Felsobuki, Nucl. Instrum. Methods Phys. Res., Sect. B **94**, 197 (1994).

[44] S. R. Coon, W. F. Calaway, M. J. Pellin, and J. M. White, Surf. Sci. **298**, 161 (1993).

[45] See the Supplemental Material at http://link.aps.org/supplemental/10.1103/PhysRevLett.113.027604, for additional presentations of the data and model predictions given in Fig. 2(b) and discussion of Ag_2 emission mechanism.

[46] K. O. E. Henriksson, K. Nordlund, and J. Keinonen, Phys. Rev. B **71**, 014117 (2005).

[47] E. Kolodney and A. Amirav, Chem. Phys. **82** 269 (1983).

[48] B. Tsipinyuk, A. Budrevich, and E. Kolodney, J. Phys. Chem. **100**, 1475 (1996).

[49] D. R. Miller, in *Atomic and Molecular Beam Methods*, edited by G. Scoles (Oxford University Press, New York, 1988), p. 14.